Pergamon

Materials Research Bulletin, Vol. 33, No. 2, pp. 237–252, 1998

0025-5408/98 $19.00 + .00

PII S0025-5408(97)00229-8

NEW SYNTHESIS ROUTE OF $PbMo_6S_8$ SUPERCONDUCTING CHEVREL PHASE FROM ULTRAFINE PRECURSOR MIXTURES: I. PbS, MoS_2 AND Mo POWDERS

Sylvie Even-Boudjada*, Laurence Burel, Roger Chevrel, and Marcel Sergent
Laboratoire de Chimie du Solide et Inorganique Moléculaire (LCSIM), UMR CNRS
6511, Université de Rennes I, Avenue du Général Leclerc, 35042 Rennes Cedex, France

(Refereed)
(Received June 30, 1997; Accepted July 2, 1997)

ABSTRACT

Fine powders of $PbMo_6S_8$ Chevrel phase (~0.5 μm) obtained from new ultrafine precursor powders present excellent intrinsic superconducting properties, such as a critical temperature, T_c, of about 14 K. These results are due to ultrafine quasi-spherical PbS, MoS_2, and Mo precursor powders (0.05–0.5 μm) of lead Chevrel phase synthesized by soft chemistry methods (precipitation, co-precipitation). Thus, a better reactivity between the grains of the mixture allows a decrease in the synthesis temperature of the resulting $PbMo_6S_8$ phase (800°C instead of 950-1000°C) required for the $PbMo_6S_8$ synthesis from the same precursor powders made by the classical ceramic route. These new Chevrel phase powders have very fine homogeneous grains with high potential surface reactivity, giving improved grain boundaries that are able to carry high current densities. *© 1998 Elsevier Science Ltd*

KEYWORDS: A. chalcogenides, B. chemical synthesis, C. electron microscopy, D. superconductivity

INTRODUCTION

The ternary molybdenum chalcogenides of the general formula $M_xMo_6X_8$ (M = 3d element, rare earth, Pb, Sn, etc., $1 \leq x \leq 4$, and X = S, Se, Te) represent a wide variety of compounds well known as Chevrel phases [1]. These materials crystallize in black microcrystalline

---

*To whom correspondence should be addressed.

powders. Some of them have outstanding superconducting properties, for example, $PbMo_6S_8$ compound (T_c: 14.5 K and Bc_2 (0) $\approx$ 70 T [2,3]).

The so-called classical ceramic synthesis of $PbMo_6S_8$ (PMS) is carried out at high temperature in sealed evacuated silica tubes. A mixture of either Pb, Mo, and S elements or PbS, Mo, and MoS_2 or Mo_2S_3 binary sulfides in good proportions is introduced into pellets or powders. Until now, PMS has generally been prepared at about 950-1000°C from PbS, Mo, and MoS_2 powders. These starting materials are synthesized from mixtures of elements and give grain sizes of about 1–15 μm with different morphologies, such as sheets for MoS_2 grains. We call them classical precursors. The grain size of the resulting PMS powders is about 5–10 μm.

Our objective is to lower the PMS grain size (~0.5–1 μm) by about one order of magnitude of that previously obtained in order to have an excellent homogeneity of the physical properties of the PMS powder grains as the intrinsic superconducting properties (T_c, Bc_2) and to have a better connectivity between grains to improve the transport properties (e.g., J_c, critical current density).

Already a new synthesis method [4,5] using soft chemistry under gas flow has allowed ultrafine PMS powder grains to be obtained. In this paper, we describe new synthesis methods for obtaining PMS ultrafine precursor powders and the PMS phase one, but without gas flow.

EXPERIMENTAL AND RESULTS

The powders were handled under inert atmosphere (argon gas) to avoid oxygen contamination, which degrades the physical properties, for instance, the T_c superconducting temperature of the resulting PMS phase [6,7].

Powder specimens were examined by X-ray diffractometry (XRD) using Cu $K\alpha_1$ radiation to identify the phases. The correction of diffraction angles was carried out using silicon as the powder standard. The grain size and the morphology of the powders were observed by scanning electron microscopy (SEM). The particle size distribution of the samples was determined by Fraunhofer diffraction, using a polarization intensity differential scattering system on a laser granulometer (Coulter LS230). The powders were dispersed in distilled water with a sodium polyphosphate dispersing agent and subjected to ultrasonics for 15 min. The results for particle distribution are represented in % volume or % number vs. the logarithmic scale of the diameter (μm) of the grain. Thus, the % volume corresponds to the volume percent occupied for each granulometric class, and the % number (deduced from the % volume result) corresponds to the number percent of grains that have the same diameter. A sample suspension containing a few large particles and many small ones will have a very important % volume repartition for small and large diameters, but it will show only a very high % number distribution for small diameters. We define d_m as the mean diameter of the one repartition peak.

Calorimetric measurements were performed with a high temperature differential microcalorimeter from 200 to 1000°C in a sealed (under partial N_2 pressure) silica tube. On a graph, we define T_i as the initial temperature of the peak, T_f as the final temperature, and T_p as the temperature of the peak maximum. The superconducting transition temperature, $T_{c(onset)}$ is measured by an AC susceptometer under a 3 mgauss AC field.

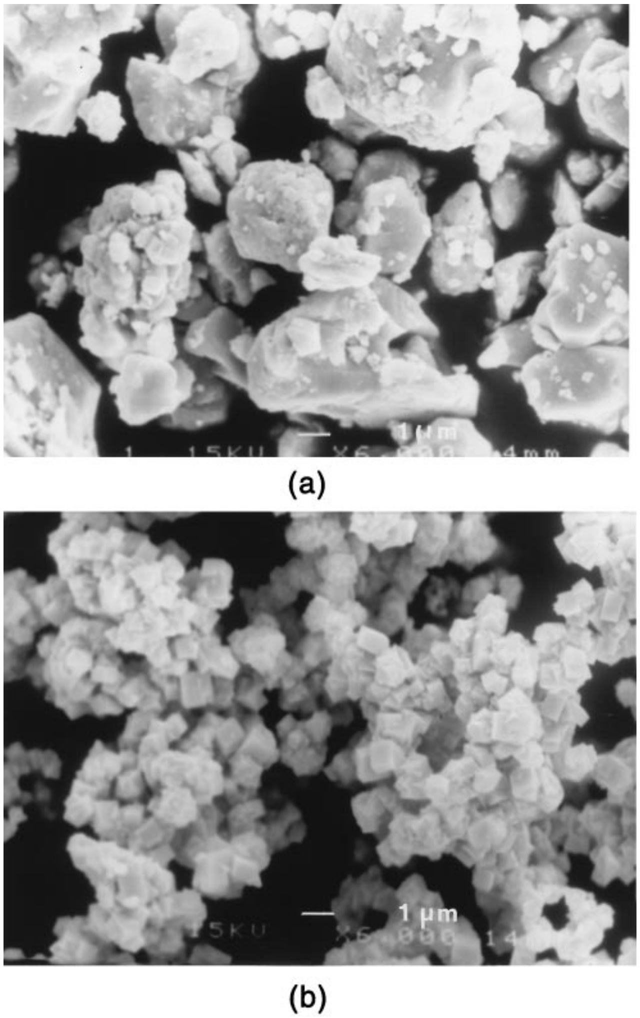

FIG. 1
SEM images of PbS powder prepared by (a) classical ceramic route (5–10 μm) and (b) new precipitated route (0.5–1.0 μm). Scalemarker in (a) represents 1 μm.

Synthesis and Characterization of Ultrafine Precursor Powders of $PbMo_6S_8$

In this section, we describe new processes for the synthesis of ultrafine precursors of the lead Chevrel phase: PbS, MoS_2, and Mo powders [8].

Ultrafine PbS powder. Until now, classical PbS powder has been prepared from lead (purity: 99.9999%) and sulfur (99.999%) elements by liquid reaction to about 350°C in a sealed evacuated glass tube. Large broken cubic-shaped crystalline gallena grains are observed, but the grain size of classical PbS powder is about 5–10 μm, according to SEM observations after sieving below 45 μm (Fig. 1a).

First, in the synthesis of ultrafine PbS powder, aqueous solutions of $Pb(NO_3)_2$ lead nitrate (99.5%) and $CS(NH_2)_2$ thiourea (99.0%) are prepared [9]. Second, both solutions are added simultaneously to a bath of sodium hydroxide (0.75 M). The resulting precipitate is filtered, washed with hot diluted HCl acid and then several times with distilled water, and finally dried under vacuum. PbS powder with a good ratio, 1:1, is obtained. PbS powder grains synthesized by precipitation present a quasi-cubic morphology and a grain size smaller than that of PbS powders prepared by the classical method [(0.5–1.0 μm vs. 5–10 μm), see Figure 1b].

PbS powder presents a particle size distribution in % volume situated mainly between 0.598 and 18.86 μm (95.61%; d_m= 5.22 μm). For the % number result, the repartition principally ranges between 0.04 and 0.598 μm (99.73%; d_m = 0.085 μm). Therefore, we can say that the suspension contains many small grains but only a few large ones.

The cubic parameters (with standard deviation) for both PbS starting materials, calculated from the XRD pattern indexing, are very close: for classical PbS powder a_{cubic} is 5.937(7) Å, for ultrafine PbS powder it is 5.926(7) Å.

Ultrafine MoS_2 powder. MoS_2, molybdenum disulfide, is a natural mineral called molybdenite. It can be prepared by direct synthesis from elements in a sealed evacuated quartz tube. We synthesized MoS_2 binary component by the classical method from commercial molybdenum (99.94%) and sulfur (99.999%) at about 720°C with the first heat treatment at 400°C. The molybdenum powder is pretreated under H_2 gas flow at 700°C. This classical preparation yields particles with a "flower" morphology. MoS_2 is not ground because of its lamellar nature; therefore, the average grain size is about 15 μm or less, after sieving at 45 μm (Fig. 2a).

To avoid the high chemical vapor pressure of sulfur, which favors the formation of large grains, we have perfected a low temperature MoS_2 preparation method that leads to ultrafine particles. This synthesis can be described as a three-step process. The first step consists of dissolving $(NH_4)_6Mo_7O_{24}\cdot 4H_2O$ ammonium heptamolybdate (99.0%) into an ammonia solution, giving ammonium monomolybdate. Thus, the sulfurization is performed by bubbling H_2S gas into the solution [10]. Large, dark-red rectangular rod-shaped crystals of $(NH_4)_2MoS_4$ ammonium thiomolybdate grow into ammonia hydrate. In the second step, after filtering, this compound is dissolved in water. By adding HCl aqueous acid into the solution, a gray-black ultrafine powder of amorphous MoS_3 is quickly precipitated. The powder is washed with distilled water to eliminate all traces of chloride and dried under vacuum. The last step corresponds with the formation of MoS_2 disulfide by decomposition of MoS_3 trisulfide at 350°C under hydrogen or nitrogen gas flow. The decomposition reaction yields ultrafine MoS_2 grains isomorphous to MoS_3 particles. They keep the same quasi-spherical morphology as that of the initial grains. Thus, the grain size of this new MoS_2 powder is about 0.1–0.5 μm (Fig. 2b), which is smaller than the size observed for classical MoS_2 powder.

The particle size distribution histogram in % volume of MoS_2 ultrafine powder is displayed in Figure 3. We observed two maxima peaks: the first one between 0.04 and 0.0926 μm (42.93%; d_m = 0.053 μm) and the second one between 0.162 and 0.657 μm (57.07%; d_m = 0.334 μm). In the inset in Figure 3, we present the repartition histogram in % number (first peak: 0.04–0.0926 μm: 99.40%; d_m = 0.050 μm). We observe that the second peak has nearly disappeared (0.60%). Other measurements under changing dispersion conditions let us conclude that the grains of 0.162–0.657 μm diameter are, in fact, an agglomerate of small grains linked by electrostatic forces of the van deer Waals type. The laser granulometry characterization elicits the SEM observation.

The XRD pattern for ultrafine MoS_2 synthesized by thermal decomposition of MoS_3

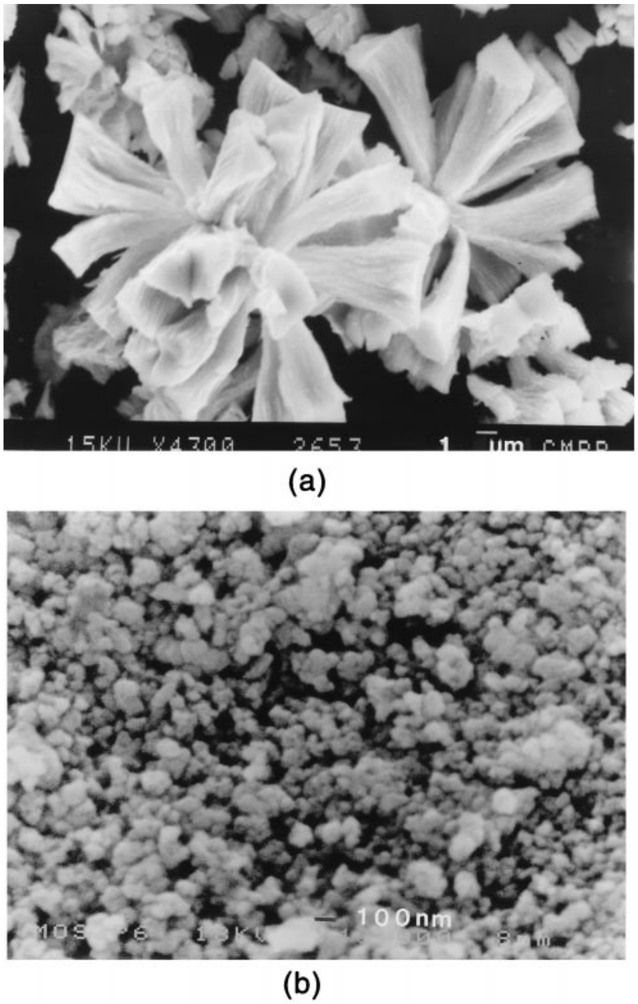

FIG. 2
SEM images of MoS_2: (a) classical powder ($\leq 15\ \mu m$) and (b) ultrafine powder arising from MoS_3 decomposition (0.1–0.5 μm). Scalemarker in (b) represents 100 nm.

exhibits a few broad peaks (2θ: ~14°, ~33°, ~39°, and ~58°), indicating a poorly crystallized compound (Fig. 4). Actually, the HREM observation of MoS_2 particles exhibits many narrow domains composed of ordered fringes (Fig. 5). These fringes characterize the lamellar nature of the MoS_2 compound, especially the Mo planes: the distance between two black fringes corresponds to 6.15 Å, equivalent to half of the *c*-hexagonal MoS_2 parameter.

Ultrafine Mo powder. Generally, commercial molybdenum powder (99.94%; 3d magnetic impurities <50 ppm) is produced from molybdenum oxides, ammonium molybdates, or molybdenite. But the grain size (1–5 μm) is greater than that of the other ultrafine precursors (PbS, MoS_2) by about one order of magnitude (Fig. 6).

We have developed a new fabrication process for preparing molybdenum powder with a

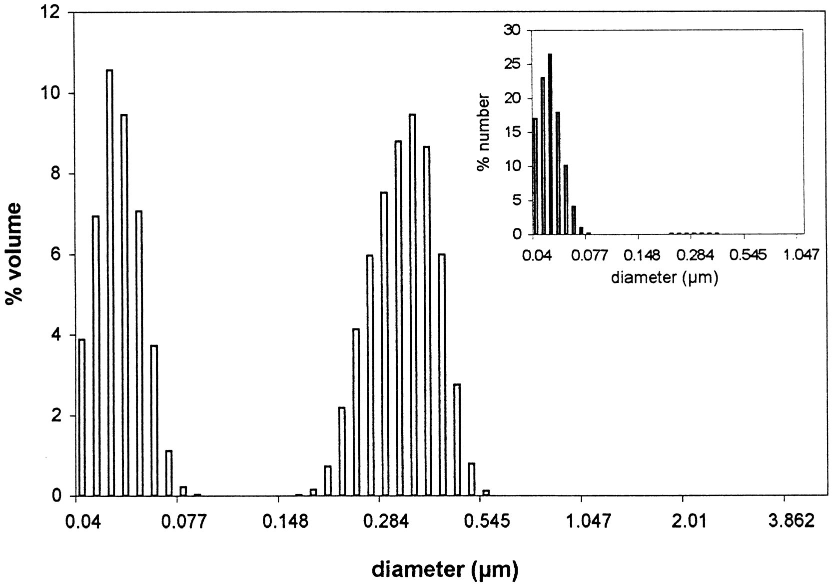

FIG. 3
Particle size distribution in % volume (laser granulometry) of MoS_2 ultrafine powder. Inset: the distribution in % number.

grain size as small as that of the other ultrafine powders. In this method, MoS_3 ultrafine powder is reduced under H_2 gas flow at 925°C.

Depending on the temperature, 925 or 945°C, for Mo synthesis, the grain size is different, but the morphology is always quasi-spherical. We have obtained an ultrafine network of

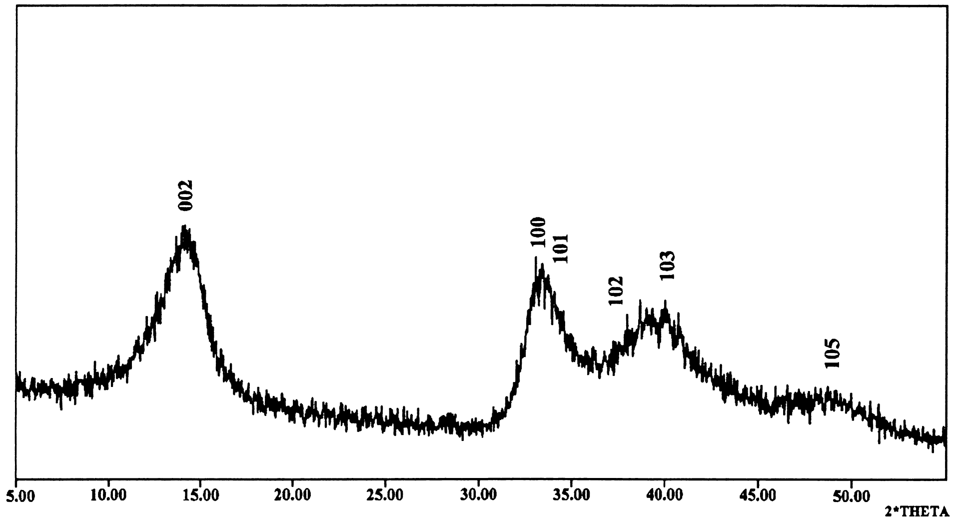

FIG. 4
XRD pattern indexed in the hexagonal system of a poorly crystallized MoS_2 ultrafine powder.

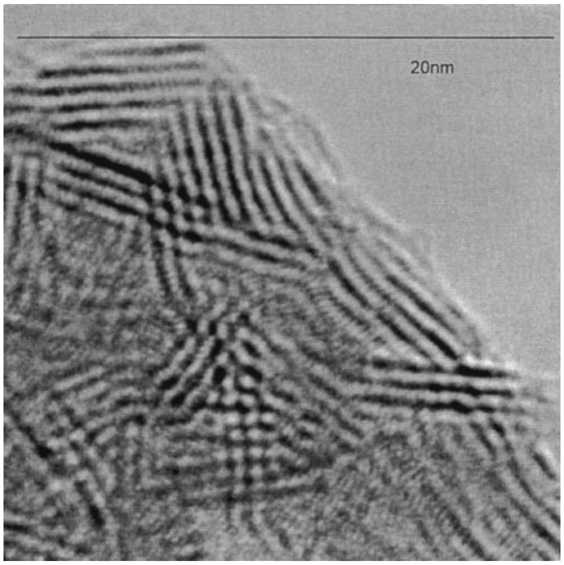

FIG. 5
HREM image of an MoS_2 ultrafine particle edge: view of narrow disordered domains of ordered fringes.

weakly interconnected particles resembling peanuts (Fig. 7). After a “manual breaking”, the grain size is about 0.3–0.5 μm for powder synthesized at 925°C (Table 1 and Fig. 8) and about 1 μm for that synthesized at 945°C.

The grain-size distribution (%vol) of molybdenum ultrafine powder presents two peaks: the first one between 0.214 and 1.261 μm (44.62%; $d_m = 0.585$ μm) and the second one between 1.261 and 4.241 μm (55.38%; $d_m = 2.411$ μm) with a global mean diameter of 1.282 μm. The result in % number shows only one peak, between 0.214 and 1.261 μm

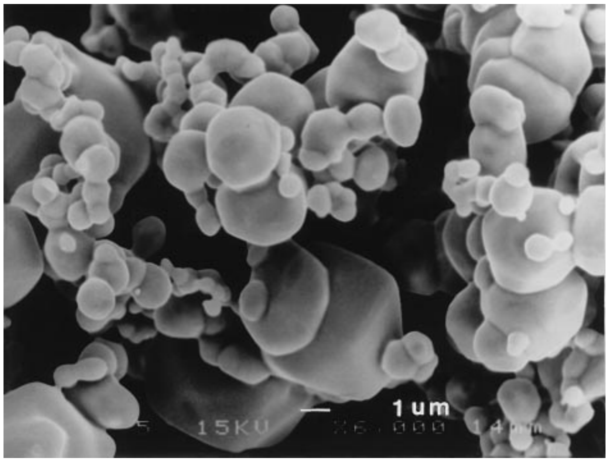

FIG. 6
SEM image of commercial Mo powder (1–5 μm).

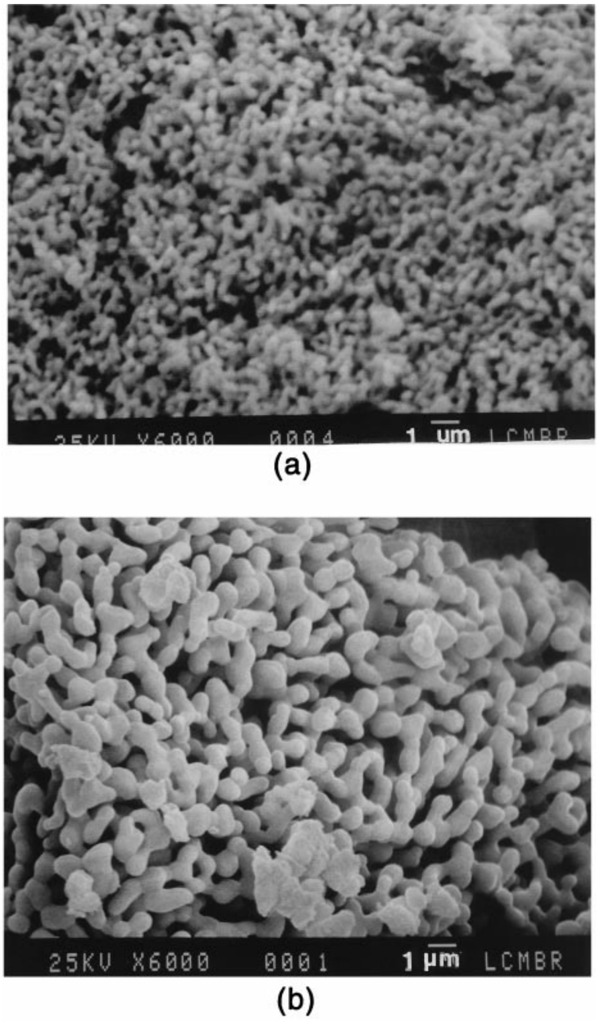

FIG. 7

SEM images of ultrafine interconnected Mo particles from MoS_3 reduction (H_2) at (a) 925°C and (b) 945°C.

(98.55%; $d_m = 0.443$ μm), indicating that the sample contains mainly small particles of these diameters.

The cubic lattice parameter, a_{cubic}, for ultrafine Mo powder is comparable to that for the commercial product: 3.150(1) Å vs. 3.147(2) Å, respectively.

Synthesis and Characterization of $PbMo_6S_8$ Phase (PbS, MoS_2, and Mo Ultrafine Precursors)

Synthesis of PMS. We have tried to understand the synthesis process of PMS compounds from the mixture of PbS, MoS_2, and Mo powders according to eq. 1, by examining the calorimetric measurements:

TABLE 1
Comparative Grain Size (SEM Observations) Between Classical and Ultrafine Precursor Powders and Mean Diameter, d_m, (% Number) of Ultrafine Powders (Laser Granulometry Measurements)

	Classical or commercial	Ultrafine	
Precursor powders	grain size (μm)	grain size (μm)	d_m (μm)
PbS	5–10	0.5–1	0.085
MoS_2	1–15	0.1–0.5	0.05
Mo	1–5	0.3–0.5	0.443

$$PbS + 3.5\ MoS_2 + 2.5\ Mo \rightarrow PbMo_6S_8 \tag{1}$$

Calorimetric measurements were performed up to 1000°C (heating rate: 8°C/h) on a mixture of classical powders. The mixture was made in an accurate order, depending on the different morphologies and grain sizes of PbS, MoS_2, and Mo classical powders: first MoS_2, then PbS, and finally Mo powders. We note that this choice corresponds, in descending order, to the volumic quantities of starting materials.

In Figure 9, we observe two thermal transitions: an exothermic effect between $T_i = 580°C$ and $T_f = 785°C$ with a maximum at $T_p = 750°C$ and an endothermic peak at $T_p = 910°C$ between $T_i = 880°C$ and $T_f = 940°C$. These two anomalies indicate that two different reactions occur during the PMS phase synthesis. These results together with XRD investigations allow us to attribute these two calorimetric peaks.

The exothermic effect is related to the following reaction between lead sulfide and molybdenum:

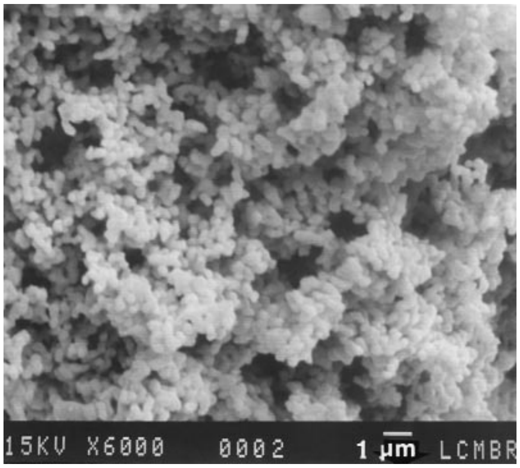

FIG. 8
SEM image of an ultrafine Mo particle (from MoS_3 reduction at 925°C) after a “manual breaking” (0.3–0.5 μm). Scalemarker represents 1 μm.

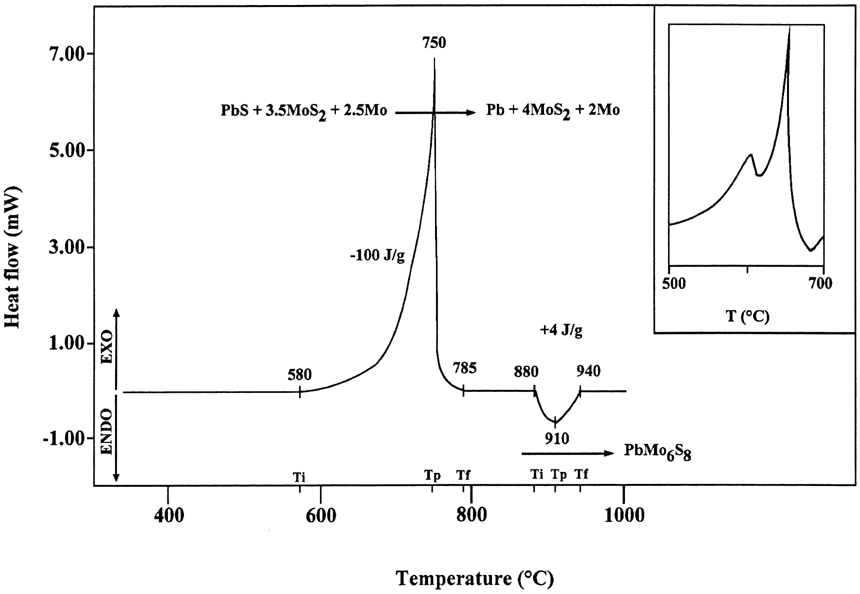

FIG. 9

Calorimetric study of $PbMo_6S_8$ formation from a mixture of classical PbS, MoS_2, and Mo powders at an 8°C/h heating rate. Inset: a study of the first exothermic peak at 3°C/h heating rate.

$$PbS + 0.5\ Mo \rightarrow Pb + 0.5\ MoS_2 \tag{2}$$

The dissipated energy for this exothermic reaction is about −100 J/g. This result is confirmed by another calorimetric study performed with only the (PbS + 0.5Mo) mixture at the same heating rate. The resulting powders are a mixture of lead metal and MoS_2 disulfide characterized by X-ray powder diffraction. The peak shape of the first transition is wide and can be modified with the heating rate (inset, Fig. 9). The presence of two peaks during this exothermic reaction (inset, Fig. 9) is due to the low heating rate (3°C/h) and can be explained by an easy chemical attack on the surface of all the Mo grains by sulfur vapor arising from the decomposition of PbS grains. At the end of this reaction, of course, many grains still have molybdenum cores. The reactivity of these grains is lowered due to this thin layer of MoS_2 at the Mo grain surface, which prevents the sulfurization. In consequence of this inertness, the sulfur pressure increases. With increasing temperature, this peel cracks and a second attack against the Mo grain cores takes place.

At high temperature ($T_p = 910°C$), the endothermic anomaly represents the reaction of PMS synthesis (eq. 3); the PMS formation is made with an enthalpy of 4 J/g.

$$Pb + 4\ MoS_2 + 2\ Mo \rightarrow PbMo_6S_8 \tag{3}$$

From classical precursors mixture. The XRD study of the PMS fabrication from these precursors shows that the compound begins to form at 800°C after 36 h of reaction. To increase the formation kinetic, the temperature was raised to, and kept at, 950°C for 24 h, leading to the formation of PMS pure phase. We think these differences of temperature with

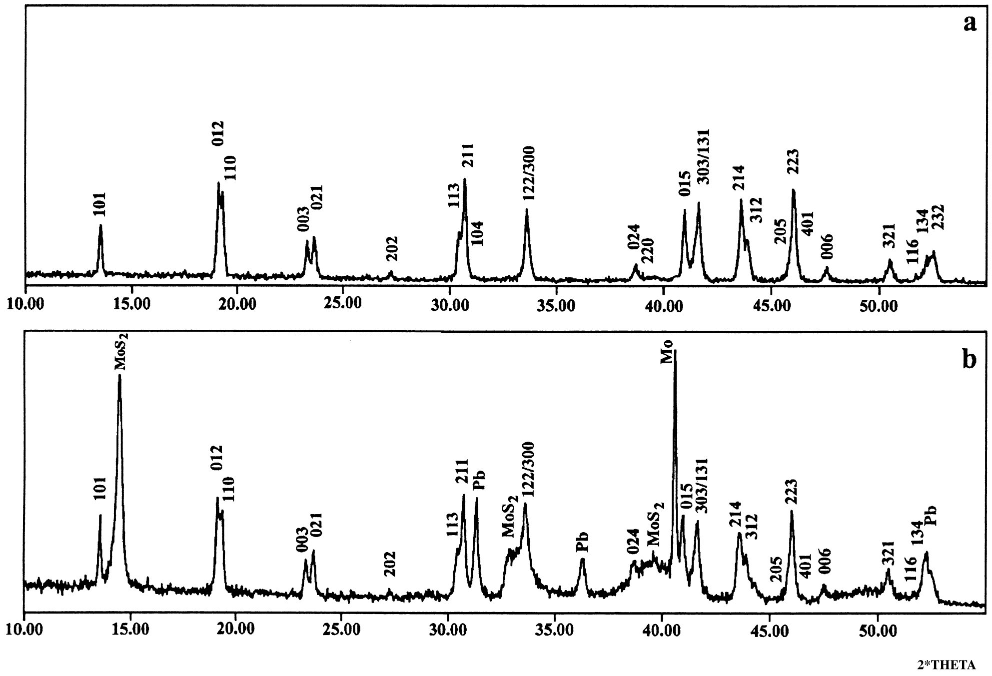

FIG. 10

XRD patterns indexed in the hexagonal system (R3) of $PbMo_6S_8$ samples obtained at 750°C/24 h plus 800°C/36 h from a mixture of (a) ultrafine precursor powders and (b) classical powders.

calorimetry results can be explained by the very high heating rate ($\sim$150°C/h $\equiv \sim$ a ramp of 5 h to final temperature) in the PMS synthesis process. The energy dissipated by the intermediate exothermic reaction (eq. 2) can be used to form the PMS phase at lower temperature, 800°C (furnace temperature). On the other hand, for calorimetry, the heating rate is very low (8°C/h), which corresponds to a ramp of about 3 days to final temperature; thus, the dissipated energy for the first reaction has no effect on the PMS fabrication.

From ultrafine precursors mixture. The same mixture of components (PbS, MoS_2, and Mo) as used for the classical powders is used here but in the state of ultrafine powders.

The XRD study shows that the $PbMo_6S_8$ phase is completely formed at 800°C after 18 h of reaction. For a comparative investigation of the classical and the ultrafine precursor syntheses, we have carried out the same heat treatments (750°C/24 h + 800°C/36 h) with the same amounts of powder in sealed evacuated silica tubes.

First, we chose the 750°C/24 h pretreatment based on the previous calorimetric result concerning the intermediate reaction between PbS and Mo components. We selected the second heat treatment, 800°C/36 h, because it was attributed to the start of PMS formation from classical powders, as viewed from the XRD investigation.

The XRD pattern obtained from ultrafine precursors (Fig. 10a), corresponds to a pure PMS phase, whereas the XRD pattern observed from the classical powders (Fig. 10b) reveals an incomplete reaction: a mixture of about 50% PMS with the presence of unreacted Pb, MoS_2, and Mo. Lead element arises from the intermediate reaction (eq. 2).

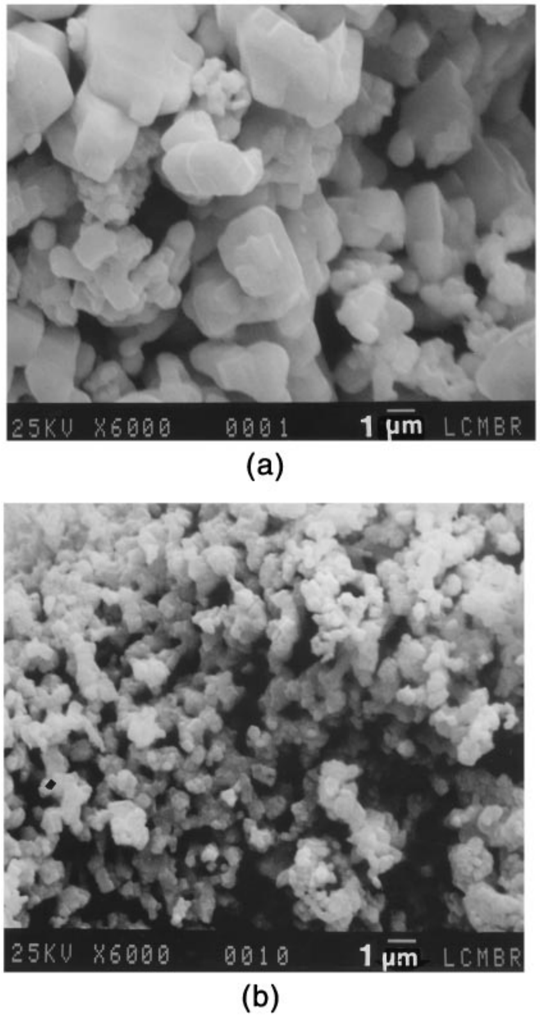

FIG. 11
SEM images of $PbMo_6S_8$ (1000°C/24 h) from mixture of (a) classical precursors (~5 μm) and (b) fine precursors (~ 0.5–1.0 μm).

Physical characterization and properties of $PbMo_6S_8$ phase. PMS phase samples from PbS, MoS_2, and Mo mixed classical and ultrafine precursor powders were uniaxially pressed under Ar atmosphere and heated at 1000°C for 24 h in sealed evacuated quartz tubes. XRD patterns reveal pure PMS phase in the samples of both precursor powders.

The grain size of the classical PMS powders, estimated from SEM observations, is about 5 μm (Fig. 11a). In comparison, the grain size of the ultrafine PMS powders is about 0.5–1 μm, i.e., one order of magnitude smaller (Fig. 11b).

The grain-size distribution (%vol) of classical PMS powders, based on laser granulometry measurements, mainly ranges from 1.149 to 24.95 μm [96.35%; $d_m = 7.232$ μm; (Fig. 12a)]. In % number, this repartition is between 1.149 and 24.95 μm (99.99%; $d_m = 3.189$ μm),

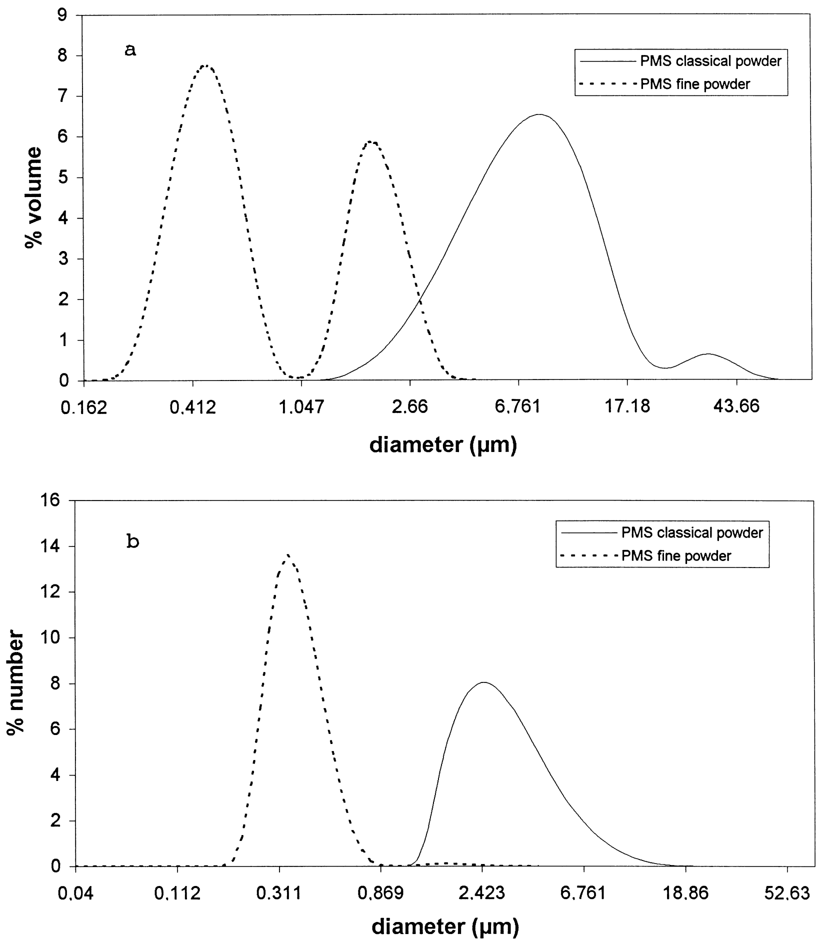

FIG. 12
Grain-size distributions of fine and classical PMS powder (a) in % volume and (b) in % number.

indicating that whole particles have grain sizes in this range (Fig. 12b). These values are summarized in Table 2.

For ultrafine PMS powders, we observe two grain-size distributions in % volume: the first peak is between 0.178 and 1.047 μm (61.29%; $d_m = 0.477$ μm) corresponding to small particles, and the second peak is between 1.047 and 4.656 μm (38.71%; $d_m = 2.10$ μm), corresponding to large particles. On the other hand, for % number distribution, one peak is displayed between 0.178 and 1.047 μm (99.33%; $d_m = 0.384$ μm), and the second peak, between 1.047 and 4.656 μm, is very weak in intensity, corresponding to 0.67 % number of particles (Fig. 12b). Thus, the PMS sample contains almost only small grains in the range of 0.178 and 1.047 μm diameter (Table 2).

As seen in Table 2, the fine $PbMo_6S_8$ powder from a mixture of ultrafine precursors presents a mean grain size one order of magnitude smaller than that of classical PMS powder.

TABLE 2
Comparative Grain Size Distributions Between Classical and Fine $PbMo_6S_8$ Powders from Laser Granulometry Measurements (see Fig. 12)

Powder	Range diameter (μm)	Volume %	Volume d_m (μm)	Number %	Number d_m (μm)
Classical PMS	1.149–24.95	96.35	7.232	99.99	3.189
	24.95–76.43	3.65	36.45	0.01	32.73
Fine PMS	0.178–1.047	61.29	0.477	99.33	0.384
	1.047–4.656	38.71	2.10	0.67	1.806

d_m: mean diameter.

These granulometric results are very close to the dimensions estimated from SEM observations.

The $PbMo_6S_8$ Chevrel phase crystallizes in a hexagonal/rhombohedral system with space group $R\bar{3}$. By X-rays powder diffraction, we determined the hexagonal parameters of the unit cell, and by inductive susceptibility measurements, we determined the superconducting critical temperature, $T_{c(onset)}$, for both samples (Fig. 13). The results are summarized in Table 3.

In Chevrel phases, there is a relationship between superconducting critical temperature and hexagonal volume of PMS phase [11]: T_c increases when the volume rises. Here, we observe the same phenomena: the highest T_c corresponds with the highest volume.

The new PMS synthesis process for ultrafine precursor powders gives the highest T_c, 14 K. As mentioned previously, both samples were subjected to the same heat treatment. In PMS phase, the highest volume corresponds to 1:6:8 stoichiometry without defects on lead and sulfur and without sulfur substitution by oxygen atoms, for instance. Here, it seems that our fine PMS phase leads to such a situation. Furthermore, the sharp transitions at the onset of

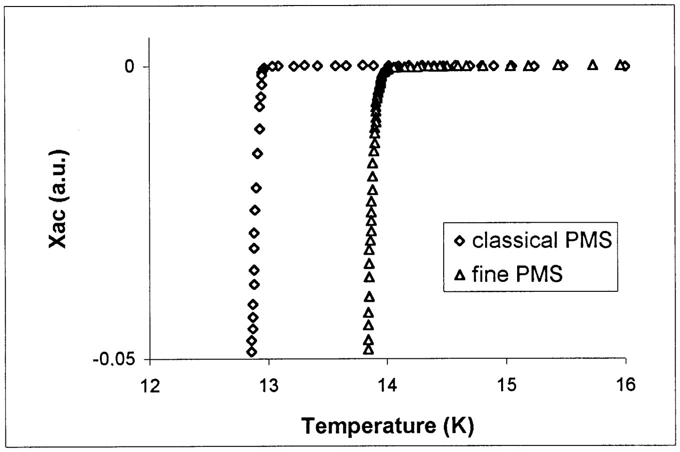

FIG. 13
χ_{AC} vs. T under 3 mgauss for both fine and classical $PbMo_6S_8$ samples.

TABLE 3
Hexagonal Unit Cell Parameters, Mean Diameter (% Number), and $T_{c(onset)}$ of PMS Prepared at 1000°C/24 h from Both Classical and Ultrafine Precursor Mixtures

PMS phase	a_H (Å)	c_H (Å)	V_H (Å^3)	d_m (μm)	$T_{c(onset)}$ (K)
Classical sample	9.209(5)	11.412(4)	838.1(7)	3.2	13.0
Ultrafine sample	9.197(3)	11.478(2)	840.8(2)	0.38	14.0

the curve, observed in Figure 13, indicate an excellent homogeneity of PMS grains in both cases.

CONCLUSION

The new synthesis processes for preparing precursor powders by precipitation and/or by a first-step liquid route allow us to obtain ultrafine quasi-spherical particles (0.05–0.5 μm). The grain size of the ultrafine precursor powders is one order of magnitude smaller, compared with the grain size of classical precursor powders, which are much more largely scattered [1–15 μm; (Table 1)]. In addition, the precursor syntheses for PbS and MoS_2 are performed at room temperature by liquid route for PbS and at 350°C for MoS_2 sulfide. The temperatures required for the fabrication of these precursors are much lower than those required for the classical precursors.

Very ultrafine precursor grains lead to a high surface area, allowing for a higher reactivity related to an easier diffusion between the powders, thus lowering the synthesis temperature of the PMS phase by about 100–150°C. Furthermore, the PMS compound from the mixture of ultrafine precursors exhibits a $T_{c(onset)}$ of 14 K, characteristic of an excellent superconducting quality of grain cores.

Before testing the current density transport capacity of these powders in future wires, new M(H) magnetization ($J_{c(calc)}$) and χ_{AC} vs. T at different alternative field measurements on highly densified bulk pellets will be performed to check the extrinsic properties of the new fine PMS powders, i.e., improvement of the connectivity between the particles and the lowering of the sintering temperature of these PMS grains.

ACKNOWLEDGMENTS

The authors thank M.P. Crosnier-Lopez, Y. Laligant, and R. Retoux of the Laboratoire des Fluorures, UPRES-A CNRS 6010, University Le Mans for their assistance with high resolution transmission electron microscopy, and J.M. Maufras of the I.U.T Lorient for calorimetric measurements.

REFERENCES

1. R. Chevrel, M. Sergent, and J. Prigent, *J. Solid State Chem.* **3**, 515 (1971).
2. B.T. Matthias, M. Marezio, E. Corenzwit, A.S. Cooper, and H.F. Barz, *Science* **175**, 1465 (1972).

3. Ø. Fischer, M. Decroux, S. Roth, R. Chevrel, and M. Sergent, *J. Phys. C: Solid State Phys.* **8**, L 474 (1975).
4. S. Even-Boudjada, L. Burel, V. Bouquet, R. Chevrel, M. Sergent, J.C. Jegaden, J. Cors, and M. Decroux, *Mater. Sci. Forum* **152–153**, 205 (1994).
5. P. Rabiller, M. Rabiller-Baudry, S. Even-Boudjada, L. Burel, R. Chevrel, M. Sergent, M. Decroux, J. Cors, and J.L. Maufras, *Mater. Res. Bull.* **29**, 567 (1994).
6. D.G. Hinks, J.D. Jorgensen, and H.L. Li, *Phys. Rev. Lett.* **51**, 1911 (1983).
7. P. Selvam, D. Cattani, J. Cors, M. Decroux, P. Niedermann, S. Ritter, Ø. Fisher, P. Rabiller, R. Chevrel, L. Burel, and M. Sergent, *Mater. Res. Bull.* **26**, 1151 (1991).
8. S. Even-Boudjada, Thèse d'Université, Rennes, France (1994).
9. H. Rahnamai, H.J. Gray, and J.N. Zemel, *Thin Solid Films* **69**, 374 (1980).
10. J.C. Bernard and G. Tridot, *Bull. Soc. Chem.* **5**, 810 (1961).
11. Ø. Fischer, *Appl. Phys.* **16**, 1 (1978).